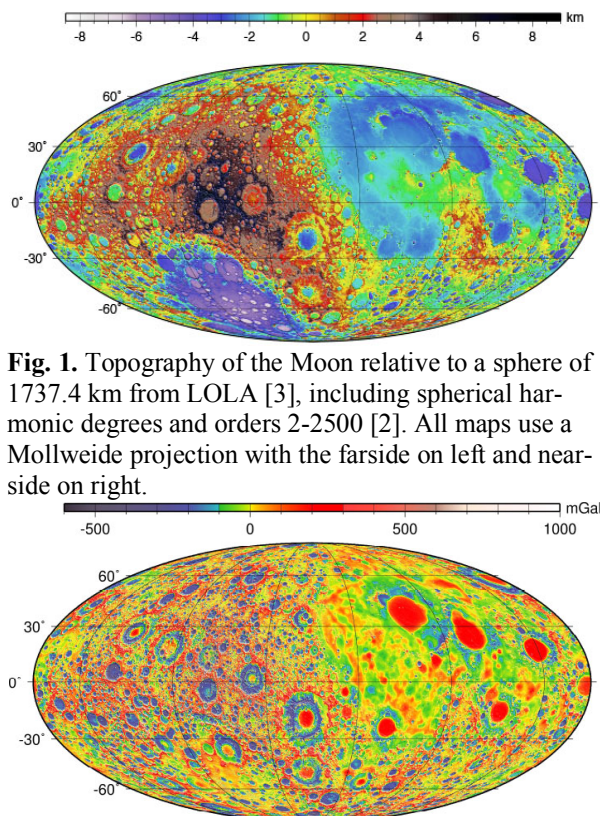
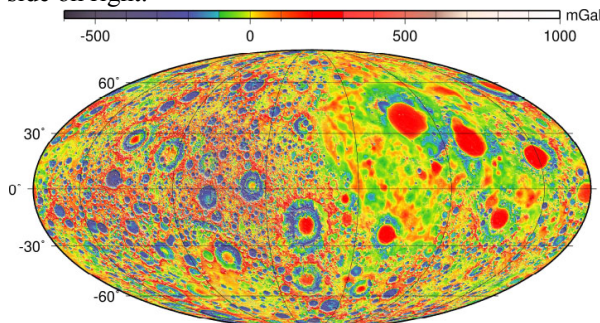


**GEOPHYSICS AND SHALLOW INTERNAL STRUCTURE OF THE MOON.** Maria T. Zuber<sup>1</sup>, <sup>1</sup>Department of Earth, Atmospheric and Planetary Sciences, Massachusetts Institute of Technology, Cambridge, MA 02139-4307, USA ([zuber@mit.edu](mailto:zuber@mit.edu)).

**Introduction:** The half century initiated with the Apollo 11 landing will go down in history as a golden age of lunar science. Here we highlight how our understanding of the Moon's thermal and tectonic evolution has been transformed by global, high-resolution geophysical data sets. Topography (Fig. 1) [1, 2] from the Lunar Orbiter Laser Altimeter (LOLA) [3] on the Lunar Reconnaissance Orbiter [4], and gravity (Fig. 2) [5, 6, 7] from the Gravity Recovery and Interior Laboratory (GRAIL) [8], supplemented by orbital geochemical mapping and Apollo sample analyses, have provided observations needed to elucidate the role of impacts and volcanism, preserved on the lunar surface and in crustal structure.



**Fig. 1.** Topography of the Moon relative to a sphere of 1737.4 km from LOLA [3], including spherical harmonic degrees and orders 2-2500 [2]. All maps use a Mollweide projection with the farside on left and nearside on right.



**Fig. 2.** Free-air gravity of the Moon from GRAIL [8], including spherical harmonic degrees and orders 7-900 [6, 7].

**Crust and Mascons:** Investigation of interior structure begins by subtracting the gravitational attraction of surface topography to produce Bouguer gravity (Fig. 3), which provides an indication of the distribution of subsurface mass anomalies. Note abundant circular regions of high positive gravity surrounded by annuli of negative gravity. These mass concentrations or

mascons [9] perturb orbits of lunar satellites. The origin of mascons has long been a conundrum in lunar science. Modeling constrained by high-resolution topography [1, 2] and gravity [5, 6, 7] determined that the anomaly pattern results from impact basin excavation and collapse followed by isostatic adjustment and cooling, and contraction of a substantial melt pool. The main parameters that influence the gravity signatures of mascon basins include impactor energy, the lunar thermal gradient at the time of impact, crustal thickness, and details of volcanic fill [10, 11].

By assuming uniform crust and mantle density, Bouguer gravity can be downward continued to an interface corresponding to the crust-mantle boundary to produce a map of crustal thickness (Fig. 4) [12]. Apparent in the map is the nearside-farside asymmetry in crustal thickness has been known since the Apollo era [13], but until the GRAIL mission global crustal thickness maps were unreliable on the farside due to the lack of direct tracking in the production of the gravitational field. Also evident is thinning of the crust beneath impact basins, which allows a definitive census of the size-frequency distribution of major impact structures [14].

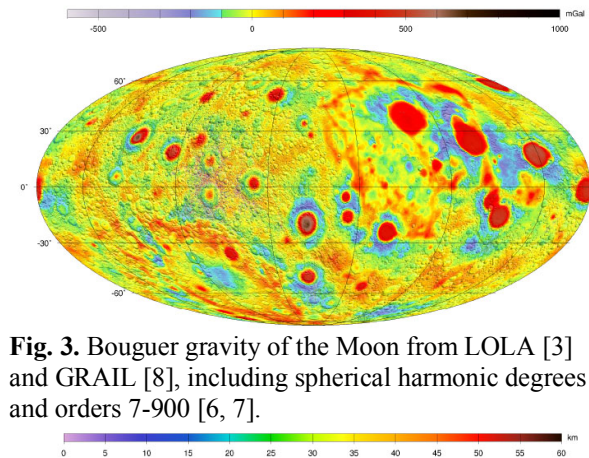


**Fig. 3.** Bouguer gravity of the Moon from LOLA [3] and GRAIL [8], including spherical harmonic degrees and orders 7-900 [6, 7].

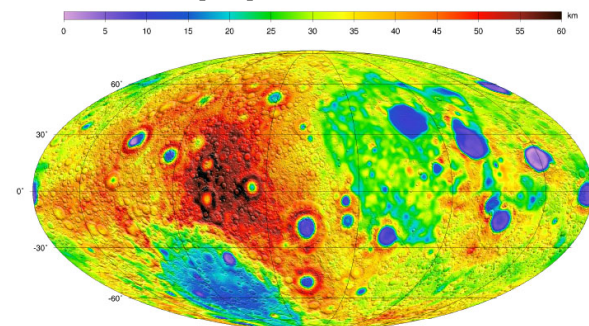


**Fig. 4.** Crustal thickness of the Moon from LOLA [3] and GRAIL [8], including spherical harmonic degrees and orders 2-900 [updated from 12].

**Pervasive Fracturing:** Minimization of Bouguer gravity indicates that the bulk density of lunar highlands crust is  $2550 \text{ kg m}^{-3}$ , substantially lower than previously assumed [cf., 15, 16]. Combined with remote sensing and sample data, this density implies an average crustal porosity of 12% within the uppermost crust [12]. Porosity variations correlate with major impact basins, whereas spatial variations in crustal density correlate with crustal composition. The crustal model has a mean thickness of 34-43 km and satisfies Apollo seismic constraints [17]. With refined crustal volume the bulk refractory element composition of the Moon is not required to be enriched with respect to Earth [12].

The low crustal density and high average porosity represent evidence for a crust pervasively fractured by impacts. Additional evidence comes from the coherence between gravity and topography (Fig. 5), the gravity divided by gravity assuming the entire signal comes from topography. The high coherence at spatial scales smaller than impact basins shows that <2% of gravity comes from subsurface sources, indicating substantial impact-related homogenization of the crust [5].

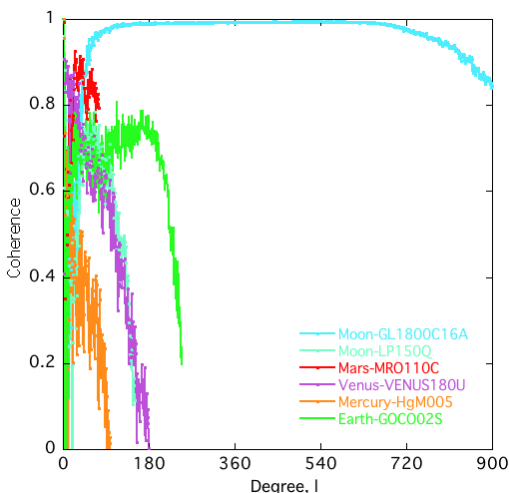


**Fig. 5.** Coherence between gravity and topography for the Moon and terrestrial planets [updated from 5].

**Giant Dikes:** GRAIL gravity gradiometry has revealed a population of linear gravity anomalies, not visible at the surface, with lengths of hundreds of kilometers (Fig. 6). These structures have been interpreted to be ancient dikes formed by a combination of magmatism lithospheric extension [18]. Crosscutting relationships indicate pre-Nectarian to Nectarian age, preceding the end of heavy bombardment. The distribution, orientation, and dimensions of the dikes suggest a globally extensional stress state arising from an increase in the Moon's radius by 0.6 to 4.9 kilometers early in lunar history, predicted by thermal models [19].

Massive dikes, formed by cooling of an ancient, hemisphere-scale nearside plume, similarly bound the

nearside maria [20], and represent conduits for magma extruded to form the maria basalts.

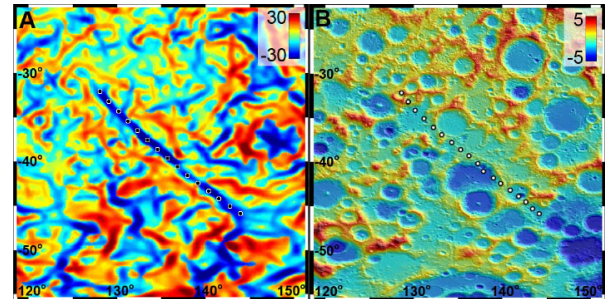


**Fig. 6.** (A) Horizontal Bouguer gradient (in Eötvös units) and (B) LOLA topography (in km) in the vicinity of a linear gravity anomaly [adapted from 18].

**The Future:** The high-resolution of the combined LOLA and GRAIL data sets have opened the opportunity to directly tie geophysical structures and phenomena to geological phenomena at the lunar surface. Using current and future data sets, there is abundant future opportunity for analyses that contribute to a holistic understanding of the evolution of Earth's fascinating natural satellite.

**References:** [1] Smith D. E. et al. (2010) *Geophys. Res. Lett.*, 37, doi: 10.1029/2010GL043751. [2] Smith D. E. et al. (2016) *Icarus*, 283, 70-91, doi: 10.1016/j.icarus.2016.06.006. [3] Smith, D. E. et al. (2010) *Space Sci. Rev.*, 150, doi: 10.1007/s11214-009-9512-y, 209-24. [4] Chin, G., S. et al. (2007) *Space Sci. Rev.*, 129, doi:10.1007/s11214-007-9153-y. [5] Zuber M. T. et al. (2013) *Science* 339, 668-671, doi:10.1126/science.1231507. [6] Konopliv A. S. et al. (2014) *Geophys. Res. Lett.*, 41, 1452-1458, doi: 10.1002/2013GL059066. [7] Lemoine F. G. et al. (2014) *Geophys. Res. Lett.*, 41, 3382-3389, doi: 10.1002/2014GL060027. [8] Zuber M. T. et al. (2013) *Space Sci. Rev.*, doi:10.1007/s11214-012-9952-7. [9] Muller, P. M. and Sjogren, W. L. (1968) *Science*, 161, 680-684. [10] Melosh H. J. et al. (2013) *Science*, 340, 1552-1555. doi: 10.1126/science.1235768. [11] Freed A. M. et al. (2014) *J. Geophys. Res.*, 119, 2378-2397, doi: 10.1002/2014JE004657. [12] Wieczorek M. A. et al. (2013) *Science* 339, 671-675, doi: 10.1126/science.1231530. [13] Kaula W. M. et al. (1972) *Proc. Lunar Sci. Conf.*, 3<sup>rd</sup>, 2189-2204. [14] Neumann G. A. et al. (2015) *Sci. Adv.*, 1, doi: 10.1126/sciadv.1500852. [15] Zuber M. T. et al. (1984) *Science*, 266, 1839-1843. [16] Neumann G. A. et al. (1996) *J. Geophys. Res.*, 101, 16,841-16,863. [17] Lognonné, P. et al. (2003) *Earth Planet. Sci. Lett.*, 211, 27-44 (2003). [18] Andrews-Hanna J. C. et al. (2013) *Science*, 339, 675-678, doi: 10.1126/science.1231753. [19] Solomon S. C. (1979) *Phys. Earth Planet. Int.*, 84, 135-145. [20] Andrews-Hanna, J. C. et al. (2014) *Nature*, 514, 68-71, doi: 10.1038/nature13697.